Geology of the Zicavo Metamorphic Complex, southern Corsica (France)

Lorenzo Dulcetta, Michel Faure, Philippe Rossi, Gabriele Cruciani & Marcello Franceschelli

View supplementary material ⧉

Published online: 17 Oct 2023.

Submit your article to this journal ⧉

View related articles ⧉

View Crossmark data ⧉

Taylor & Francis
Taylor & Francis Group

SCIENCE

OPEN ACCESS

Check for updates

Geology of the Zicavo Metamorphic Complex, southern Corsica (France)

Lorenzo Dulcetta [a], Michel Faure [b], Philippe Rossi [c], Gabriele Cruciani [a] and Marcello Franceschelli [a]

[a]Department of Chemical and Geological Sciences, University of Cagliari, Monserrato, Italy; [b]Earth Sciences Institute, University of Orléans, Orléans, France; [c]Commission for the Geological Map of the World, Paris, France

ABSTRACT

In this study, we investigated the Zicavo Metamorphic Complex (southern Corsica), which is part of the innermost Axial Zone of the Corsica-Sardinia Variscan belt. To better evaluate its geological and structural outline, a 1:5000 geological map, coupled with new structural/ microstructural and petrographic data, is presented. The complex is formed by three tectonic units, from bottom to top: (i) an Orthogneiss Unit, (ii) a Leptyno-Amphibolite Unit, and (iii) a Micaschist Unit. They are separated by ductile shear zones with a top-to-the-SE sense of shear. They underwent a polyphase deformation and polymetamorphic history, with a shortening stage in the amphibolite facies, responsible for the main structures and shearing, followed by an exhumation phase.

1. Introduction

The Variscan chain of Europe is the result of the convergence between the Gondwana and Laurussia continents, and intervening microcontinents, in the Devonian – Carboniferous time span. In spite of a huge amount of Variscan plutons, the Corsica-Sardinia Variscan belt represents one of the most complete transepts of the chain exposed in southern Europe (Carmignani et al., 1994; Rossi et al., 2009). It consists, from the SW towards the N-NE (Carmignani et al., 2001), of (1) a low-grade External Zone (or Foreland) in South-western Sardinia, (2) a low- to medium-grade Nappe Zone in central and North-western Sardinia, and (3) a high-grade Axial Zone (or Hinterland) in North-eastern Sardinia and Corsica (Faure et al., 2014).

In southern Corsica, a few km²-wide metamorphic complex, here referred to as the Zicavo Metamorphic Complex (ZMC), consists of a thick pile of Variscan metamorphic rocks. In this contribution, we present a detailed 1:5000 geological-structural map (Main Map), implemented with microstructural and petrographic-mineralogical data. The aim is to describe, through a multidisciplinary field – structural – petrographic approach, a scarcely studied portion of the metamorphic basement from Corsica, to improve our understanding regarding the complex puzzle of the Variscan chain of southern Europe.

2. Geological setting

The Corsica Island is divided into two different geological realms, namely: the Variscan Corsica in the West, and the Alpine Corsica in the North-East (Figure 1); The Alpine Corsica mainly consists of ophiolites, oceanic sediments and continental slices linked to the Cenozoic subduction and closure of the Mesozoic Liguro-Piemonte Ocean (Di Rosa et al., 2019; Vitale Brovarone et al., 2013) during the formation of the Alpine chain.

The Variscan Corsica can be considered as the innermost part of the Axial Zone of the Corsica-Sardinia Variscan belt (Cruciani et al., 2021). It can be further divided into two parts: the Corsica-Sardinia batholith, that made up most of the island, and relicts metamorphic septa (Figure 1). The metamorphic part has been divided into four domains, which group these septa, according to Faure et al. (2014) and Faure and Ferrière (2022), namely: (i) a western domain (WD), including the southern Corsica metamorphic septa (Porto Vecchio, Fautea-Solenzara, Zicavo and Vignola-Topiti septa, Figure 1), (ii) the eastern domain (ED), which includes the Belgodere septum, and (iii) the Neoproterozoic domain consisting of the Argentella and Agriates-Tenda septa. The metasedimentary and magmatic rocks cropping out in the Argentella and Agriates-Tenda areas (northern Corsica) also underwent the Neoproterozoic Cadomian orogenesis.
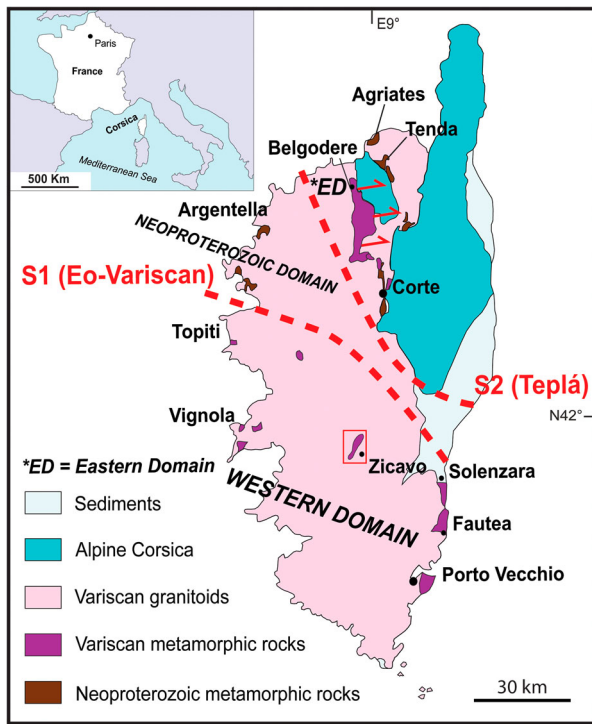
Figure 1. Schematic geological map of the Corsica island, showing the Alpine domain in the NE, and the Variscan domain in the rest of the island (modified after Massonne et al., 2018). Variscan Corsica consists of several generations of granitoids with septa of Variscan metamorphic rocks and Neoproterozoic metamorphic ones. The tectonic lines S1 and S2 (dotted red lines), interpreted as two Variscan sutures (the Eo-Variscan between N Gondwana and Armorica, and the Teplá between Armorica and the eastern Variscan domains, respectively) have been drawn according to Faure et al. (2014); the red arrows East of the Belgodere septum indicate the tectonic direction of the ductile and syn-metamorphic deformation phase in the Belgodere area.

Several authors provided petrological and geochronological data for both the metamorphism and the granitoid intrusions. Giacomini et al. (2008) obtained a 360 Ma U-Pb zircon age for the Fautea HP-HT granulites, interpreted as the age of the HP metamorphism (*c.* 1.9 GPa); a younger 340 Ma age was also obtained for the peak metamorphic conditions of the lower-pressure (0.7 GPa), middle crustal gneisses which underlie the granulites. A 320 Ma age was obtained for the dextral transpressional shear zone which put into contact the Fautea septum with the underlying Porto Vecchio one (Giacomini et al., 2008). Similar age was also reported by Massonne et al. (2018) for the metasedimentary rocks of the Porto Vecchio septum; here, garnet micaschists recorded an anticlockwise P-T path with peak pressure comparable to that of the Fautea gneisses. The migmatization (under amphibolite facies conditions) in the whole basement has been constrained at *c.* 345 Ma after leucosomes' zircon dating from different localities (Li et al., 2014). Lastly, the Corsica granitoids were emplaced during four main pulses (Paquette et al., 2003) at

345, 338, 305 and 280 Ma, separated by inactivity periods. More recently, the geochronology of the batholith has been refined by Li et al. (2014), who defined an age of 330 Ma for the first (U$_1$) Mg-K suite, and by Rossi et al. (2015); these latter authors provided ages for the second (U$_2$) and the third (U$_3$) igneous suites at 295–280 and 288 Ma, respectively.

A geodynamic reconstruction for the Corsica-Sardinia microplate was given by Rossi et al. (2009), who placed an Eo-Variscan suture in northern Sardinia and beneath northern Corsica, resulting from the Silurian-Devonian closure of the South Armorican Ocean (or Medio European Ocean, according to the recent review of Faure & Ferrière, 2022). The slab break-off would have triggered melting and mixing of lower crustal and mantle melts, with the subsequent emplacement of the first Mg-K suite. More recently, Faure et al. (2014) tried to give a consistent and exhaustive description of what could be the possible place of the Corsica basement in the framework of the European Variscan orogen. According to these authors, the above mentioned domains would be separated by two large tectonic lines (Figure 1), the S1 (WD – Argentella) and S2 (Argentella – ED) lines, regarded by these authors as suture zones; furthermore, the ED is in contact with the Agriates-Tenda septum through a regional thrust (Faure et al., 2014). The same authors also gave a preliminary correlation of these metamorphic domains with similar ones in Europe. In this regard, the WD would represent the innermost part of the Axial Zone of the Corsica-Sardinia Variscan belt and, furthermore, would show several similarities with the Upper Gneiss Unit of the French Massif Central (FMC, Faure et al., 2009).

2.1. Previous works in the ZMC

A first outline about the geology of the Zicavo area was provided through a preliminary, small scale geological map (with included the ZMC), mainly focused on the surrounding plutonic rocks, further implemented with petrographic, mineralogical and geochemical data (Vézat, 1986, 1988); This author distinguished three lithological series, from bottom to top: a gneiss, an amphibolite and a micaschist sequence. Later, Thevoux-Chabuel et al. (1995) gave a new overview of the ZMC; they provided a first structural and deformative description, discriminating two different deformation phases, D$_1$ and D$_2$. The D$_1$ phase would be characterized by an S$_1$ foliation and an L$_1$ lineation, which apparently did not affect the entire gneissic unit; a top-to-the-SW sense of shear would be linked to this phase. It developed at medium pressures with blastesis of kyanite in the sedimentary intercalations of the amphibolite sequence. The D$_2$ phase developed at HT-LP conditions, forming the main structures (S$_2$ foliation and L$_2$ lineation) and featured by a top-to-

the-SE shearing. Thevoux-Chabuel et al. (1995) interpreted these two phases linked to the main collision and crustal thickening of the orogen, and to the subsequent extensional collapse, respectively. Based on these latter findings, Gardien et al. (1997) presented a preliminary P-T metamorphic evolution, describing a clockwise path with peak pressures characterized by kyanite occurrence, and peak temperatures of 600–650°C; these authors related the HT evolution to the late crustal thinning associated with granitoid intrusion. Faure et al. (2014) described the three sequences in terms of litho-tectonic units, recognizing two shear zones which highlight the contacts between them. Moreover, for the first time, a 336 Ma age from monazite U-Pb dating from the micaschists was provided, interpreted as the age of the Variscan metamorphism (Faure et al., 2014). About further geochronology, an age of 458 ± 32 Ma in the orthogneiss was obtained after zircon U-Pb dating, and interpreted as the protolith age (Rouire et al., 2014), while the granitoids surrounding the metamorphic complex provided ages of c. 297 Ma (Rossi et al., 2012).

3. Methods

The mapped area is localized in southern Corsica, covering an area of ~24 km^2 within the Corse-du-Sud Department of France, between the Zicavo, Cozzano, Giovicacce and Bagnes de Guitera Municipalities. The topographic maps used during field surveys have been acquired from the French Géoportail database. The 10 m cell size grid resolution Digital Terrain Model (DTM) of Corsica has been acquired from the Corsica Géoportail and has been used for subsequent digitalization of the Main Map within the QGIS environment after extraction of new 10m-spaced contour lines. The used spatial files were georeferenced in the WGS 84 – UTM Zone 32 T reference system. The Main Map is at the 1:5000 scale. Structural and microstructural elements (foliation, lineation) have been classified according to Passchier and Trouw (2005) and Piazolo and Passchier (2002). Mylonites have been classified according to the matrix percentage with respect to the porphyroclasts in: protomylonites (matrix ≤50%), mylonites (50–90%), and ultramylonites (≥90%) (Fossen, 2016). Microstructural investigations and semi-quantitative mineral chemistry were carried out using a FEI Quanta 200 Scanning Electron Microscope at Centro Servizi d'Ateneo per la Ricerca (CeSAR), University of Cagliari.

4. Tectonic units

The ZMC is formed by three tectonic units. Geometrically, from bottom to top (and from SW to NE, Figure 2), they are: (1) the Orthogneiss Unit (OU), (2) the Leptyno-Amphibolite Unit (LAU); and (3) the Micaschist Unit (MU). In the following, a detailed description of the units from field, petrographic and structural points of view will be provided.

4.1. The Orthogneiss Unit

The OU consists of three distinct lithologies, namely: (1) a mylonitic – ultramylonitic orthogneiss, (2) a mylonitic augen gneiss, and (3) garnet paragneiss.

Mylonitic – ultramylonitic orthogneiss − The lowermost part of the OU is represented by the mylonitic – ultramylonitic orthogneiss, which mainly outcrops along the *Taravu* riverbed in the South-western sector of the mapped area, along the D757 road between Bagnes de Guitera and *U Vergaju*, or in the slopes eastward of locality *Rossalmu*, forming two NE-SW-striking bodies surrounded and partially obliterated by granitoids. It is formed by white-gray, medium- to fine-grained (sub-millimetric) strongly foliated and folded gneisses (Figure 3(a)), characterized by stretched, mm-thick recrystallized Qz-ribbons interlayered with polycrystalline K-feldspar and plagioclase (X_{Ab} ~ 0.96) ribbons (Figure 4(a)); coarse-grained white micas are scattered in between the two domains, while retrograde fine-grained micas and chlorite can be recognized aligned with limbs of late folds. The orthogneiss becomes ultramylonitic southwestward. The protolith of the Zicavo ultramylonitic orthogneiss has been dated at 458 Ma by Rouire et al. (2014); similar ages have been obtained in the Sardinia Variscan chain. For instance, the Lodé and the Tanaunella orthogneisses in NE Sardinia have been dated at 456 and 458 Ma, respectively (Helbing & Tiepolo, 2005), while the Golfo Aranci orthogneiss provided ages between 464 and 469 Ma (Giacomini et al., 2006). The orthogneisses in NE Sardinia have been interpreted as the result of the calcalkaline igneous activity which characterized the northern Gondwana margin in the Ordovician.

Mylonitic augen gneiss − Geometrically above, the mylonitic augen gneiss crops out as a coarse-grained, few tens meter-thick body. It consists of cm-sized quartz and K-feldspar porphyroclasts, surrounded by a fine-grained, sub-millimetric Qz + Wmca + Chl matrix (Figures 3(b) and 4(b)); this facies mainly outcrops in some transepts along the Zicavo − *U Vergaju* D757a road, and sporadically in the woods South-West of Zicavo. The transition between the two different orthogneisses is gradational, and can be observed in the slopes North-East of locality *Rossalmu*. There, outcrops are mainly formed by the ultramylonitic orthogneiss, but a northward gradual increase in the percentage of quartz and feldspar porphyroclasts can be observed, towards the augen gneiss.

Garnet paragneiss − The paragneisses (Figure 3(c)) are brownish rocks that surround the orthogneisses
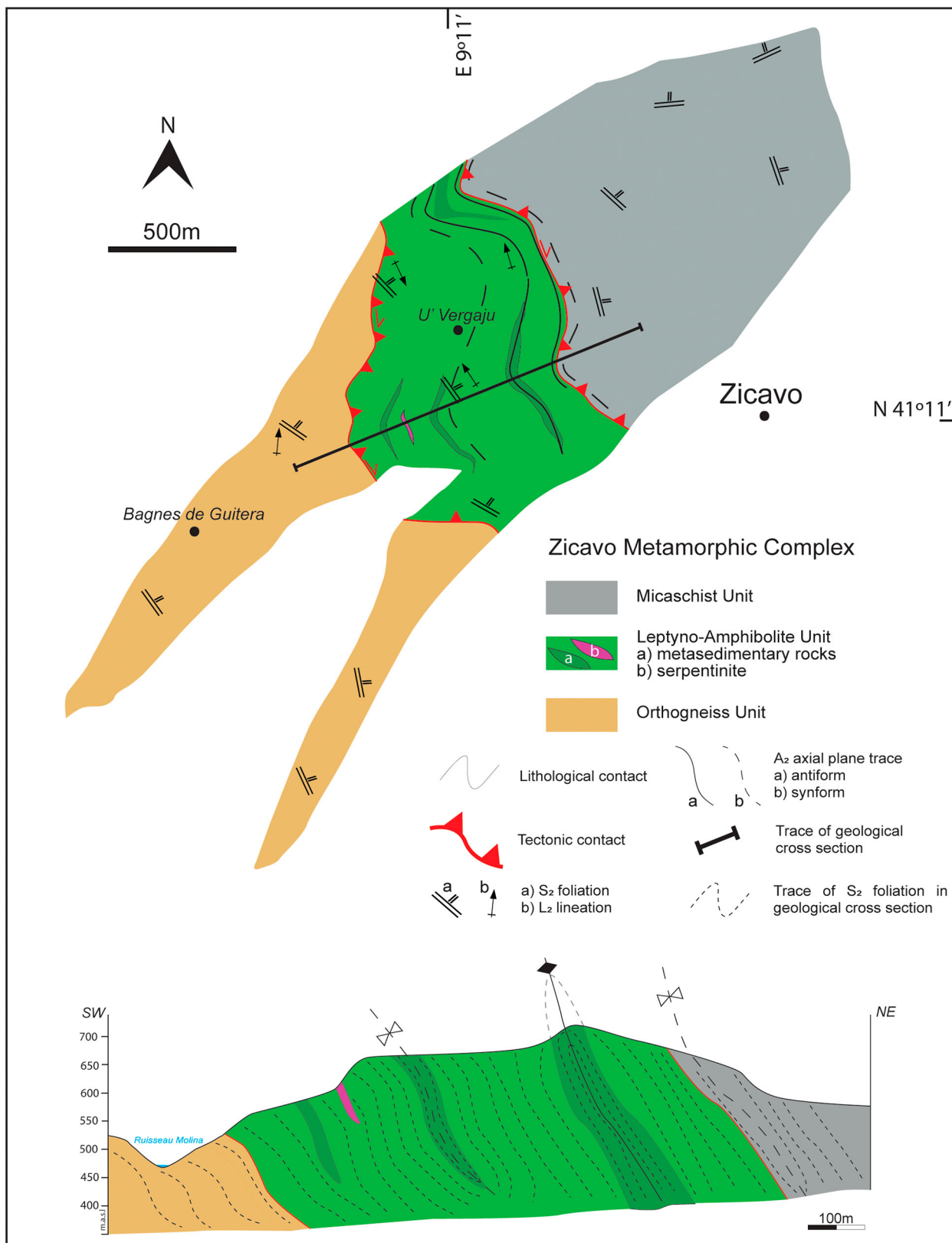
Figure 2. Simplified geological map of the Zicavo Metamorphic Complex showing the main units and the main structural features of the D₂ phase (foliation, lineation, axial plane traces) with a NE-SW geological cross section drawn perpendicular to the main structures.

and can only be recognized within some private fields along the western side of the *Taravu* river, in *Mela Frisciata* locality. The transition between the ortho- and the paragneiss is recognizable as a moderately dipping, tectonized contact. These rocks could thus

be interpreted either as the country rock or as the post-intrusion cover of the granitic protolith of the orthogneiss. These gneisses are formed by sub-millimetric subhedral garnets (Figure 4(c)) wrapped by a matrix consisting of biotite ($X_{Mg} = 0.40-0.45$),
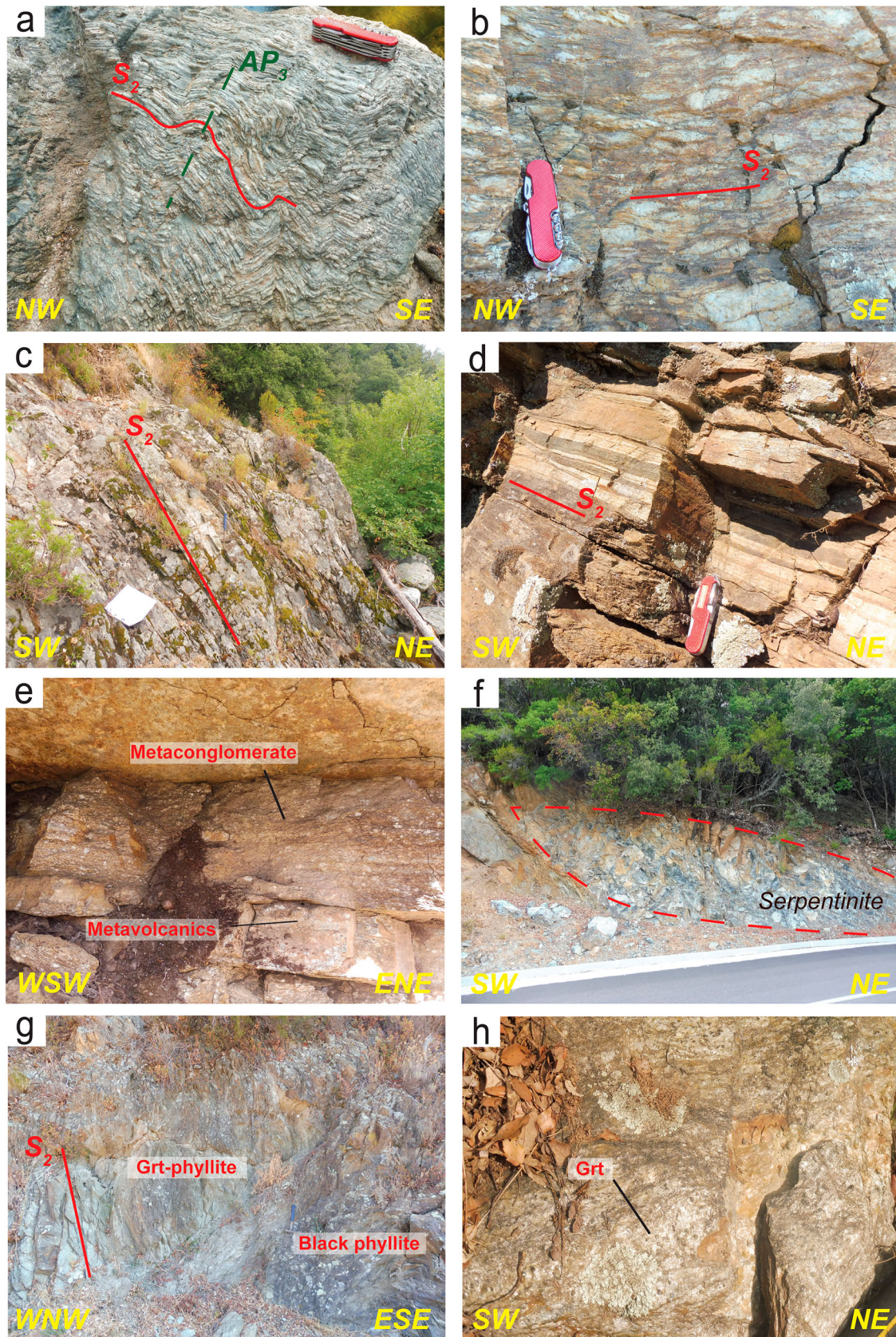
Figure 3. Field appearance of lithologies from the ZMC. (a) Folded quartz- and feldspar-rich ribbons in the ultramylonitic orthogneiss along the *Taravu* river, East of Bagnes de Guitera. (b) Mylonitic augen gneiss with quartz porphyroclasts surrounded by a fine-grained brownish matrix, from the roadcuts along the D757a road. (c) Paragneiss from the OU cropping out West of the *Taravu* river in the *Mela Frisciata* locality. (d) Intercalation of metabasites (dark layers) and 'leptynites' (white layers) from the LAU in a roadcut along the D757a road. (e) Metaconglomerate from the LAU with quartz and feldspar pebbles in a fine-grained matrix along the D757a road. (f) NE-dipping serpentinite lens embedded in basic metavolcanic rocks from the LAU along the D757a road. (g) Brittle, NW-dipping shear zone, perhaps accommodated by a previous lithological boundary between green and black phyllites in the MU, from a roadcut in locality *Gierbarella*. (h) Field appearance of the Grt-St-micaschists from the MU with millimetric to centimetric garnets in a white mica-rich matrix.

Figure 4. Microstructural features of rock samples from the ZMC. Mineral abbreviations are from Whitney and Evans (2010), except for white mica (Wmca). (a) Photomicrograph of the ultramylonitic orthogneiss from the OU; quartz and feldspar ribbons are interlayered and oriented following the main S_2 foliation, this latter folded by an F_3 fold (AP = Axial Plane). Quartz grains show a GBM recrystallization mechanism. CP (=crossed polars). (b) Evidence for a top-to-the-SE se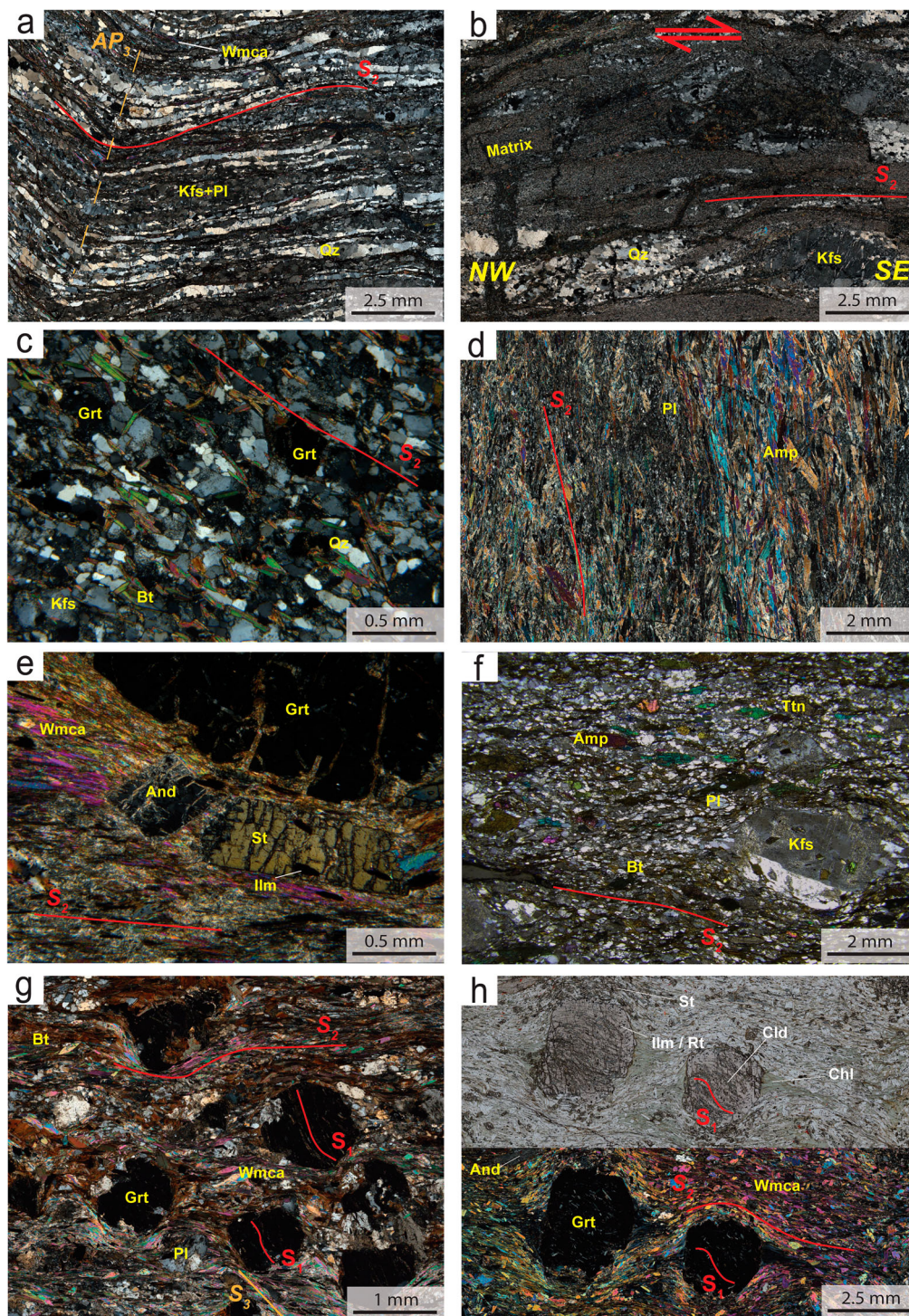nse of shear associated with the main S_2 in the mylonitic augen gneiss. K-feldspar (lower right) shows asymmetric mantles, while recrystallized quartz aggregates are sheared. The fine grained matrix is formed by Qz + Wmca + Chl. Red arrows highlight the shear sense. CP. (c) Photomicrograph of a garnet-bearing paragneiss from the OU; biotite crystals are aligned following the S_2 foliation. The S_2 apparently wraps sub-millimetric garnets, together with quartz and K-feldspar. Fine-grained micas grow on feldspars. CP. (d) Photomicrograph of an amphibolite from the LAU; green amphibole represents >80% of the rock, while plagioclase is subordinate to small microdomains. CP. (e) Evidence for syn-kinematic staurolite and post-kinematic andalusite in a Grt-micaschist from the LAU. (f) Photomicrograph of the metaconglomerate from the LAU. The larger clasts are made up of K-feldspar with included white mica and biotite; the matrix is composed by Bt + Pl and envelops millimetric amphibole and titanite. CP. (g) Photomicrograph of a Grt-Bt-micaschist from the MU. Garnet and (zoned) plagioclase are wrapped by a Bt + Wmca + Qz + Ilm matrix; chlorite grows in garnet strain shadows or on prograde biotite crystals. CP. (h) Photomicrograph of a garnet-staurolite micaschist from the MU. Garnet reaches several millimeters in size and contains inclusions of Cld + Rt + Wmca + Ilm; garnet is wrapped by a matrix consisting of Wmca + Chl + St + Qz + Pl + Ilm. The photomicrograph is shown both in plane-polarized light and crossed polars.

zoned plagioclase (X_{Ab} = 0.74–0.64 from core to rim), ilmenite, quartz, apatite and zircon. Garnet is slightly zoned, with the manganese component increasing towards the rim ($Alm_{78}Sps_5Prp_{10}Grs_7$ – $Alm_{74}Sps_{14}Prp_7Grs_5$ from core to rim, respectively). Inclusions in garnet are represented by ilmenite, zircon, apatite, monazite and quartz.

4.2. The Leptyno-Amphibolite Unit

The LAU is a thick metavolcanic sequence with subordinate metasedimentary intercalations (Figure 2). Three rock types have been detected forming this unit: (1) metavolcanic rocks, (2) metasedimentary rocks, and (3) serpentinite.

Metavolcanic rocks − The metavolcanics are characterized by interlayered metabasites and quartz-feldspathic ('leptynites') gneisses, whose layers range from plurimetric to centimetric in thickness (Figure 3(d)). The metabasites are represented by amphibolites and banded amphibolites (layers in these latter are discriminated by the relative amount of amphibole and plagioclase), sometimes with >80% of green amphibole (mainly actinolite, rimmed by hornblende) and subordinate zoned plagioclase (X_{Ab} = 0.60–0.50 / 0.49 from core to rim) (Figure 4(d)); other phases include apatite, ilmenite, epidote (sometimes included in amphibole), quartz and albite. The leptynites are whitish metarhyolites consisting of Qz + Kfs + Ab + Wmca + Ap ± Zrn ± Ep, and retrograde chlorite; albite is almost pure ($X_{Ab} \sim 0.96$), whereas white mica X_{Mg} is about 0.48–0.49. Moving structurally upward in the unit, the amount of interlayered leptynites apparently decreases. These two types of metavolcanic rocks, and the LAU as a whole, largely outcrop along the D757a road and in the surrounding reliefs. Also, plurimetric interlayering of acid-basic metavolcanics have been detected along the *U Vergaju* – Cozzano D757 road-cuts, before the contact with the MU.

Metasedimentary rocks − The metasedimentary intercalations of the LAU are Grt-bearing micaschists, fine-grained phyllites and metagreywackes, and meta-conglomerates. The former outcrop in the slopes surrounding the D757a road and consist of a NE-dipping micaschist lens wherein centimetric garnets are wrapped by a Wmca + Bt + St + Qz + Chl ± Ilm matrix (Figure 4(e)); the compositionally zoned garnet ($Alm_{69}Sps_{11}Prp_5Grs_{15}$ – $Alm_{81}Sps_6Prp_5Grs_8$ from core to rim) preserves Ilm + Chl + Qz inclusions. Post-kinematic andalusite has also been detected in these rocks (Figure 4(e)). At a lower portion of the unit, near the contact with the augen gneiss, a NE-dipping feldspar-rich, Grt-Bt-metagreywacke lens crops out, formed of foliated rocks composed of Pl + Kfs + Qz + Grt + Bt + Wmca; in these rocks, garnet preserves Ep + Qz + Wmca ± Pl inclusions. The phyllites outcrop in the reliefs surrounding the *U Vergaju* –

Giovicacce D228 road; they are gray, fine-grained, mylonitized rocks. At the thin section scale, they are mainly composed of Qz + Pl + Wmca + Chl ± Bt ± Grt, with minor garnet and biotite being strongly chloritized. The metaconglomerate outcrops along the D757a road, West of Zicavo, and surrounding reliefs. It occurs as a 50–60 m-thick, NE-dipping lens of foliated conglomerates (interlayered with thin acid metavolcanic rocks layers) with variable grain size (Figure 3(e)); it has feldspathic clasts in a fine-grained arenaceous-pelitic matrix (Figure 4(f)), mainly composed of biotite (X_{Mg} = 0.46–0.48), plagioclase (X_{Ab} = 0.68–0.80), K-feldspar (X_{Na} = 0.04–0.08), and subordinate quartz, apatite, zircon, epidote, Fe-oxides; the matrix also hosts millimetric amphibole (hornblende) and titanite; retrograde chlorite grows on biotite. These rocks are probably the result of erosion and deposition of clastic material within the basin in which volcanics were emplaced.

Serpentinites − The serpentinite is observable only in one locality, a few dozen meters below the conglomerate; here, a NE-dipping, 6 / 7 m-thick lens of yellowish-black rocks crops out (Figure 3(f)), lacking any clear foliation. The lens is cut by NW-SE and E-W-striking centimetric brittle-ductile shear zones parallel to the foliation of surrounding metavolcanics, and appears in contact with the enveloping amphibolites through ductile, NW-SE-striking cm-thick ductile shear zones. This rock is composed of two different domains: an inner part, which appears black in the field, and an outer yellowish part, with millimetric thickness, that rims the first one. From a petrographic point of view, both the inner and the outer parts are formed by serpentine group minerals, chlorite, and magnetite, with a typical mesh-structure. These rocks were described by Rouire et al. (2014) as meta-harzburgites on the basis of pyroxene and olivine relics. Similar rocks have also been detected in the Topiti septum in western Corsica (Tommasini, 1993) and described as meta-harzburgites as well.

4.3. The Micaschists Unit

The (structural) top of the ZMC is featured by the MU (Figure 2), which is a metapelitic sequence mainly formed by Grt-Bt-phyllites and schists, even if Grt-St-micaschists have been detected in a very restricted outcrop near the contact with the LAU. The grain size of the rocks in the MU increases moving towards the LAU. Intercalated in the sequence there are few lenses of black phyllites, with associated very thin layers of quartz-phyllites. The unit extensively outcrops along the *U Vergaju* – Cozzano D757 road and the *U Vergaju* – Giovicacce D228 road.

All analyzed samples from this Unit show the main assemblage Grt + Chl + Wmca + Bt + Qz + Pl +

Ilm but with differences in grain size, amount of biotite and plagioclase, and composition of this latter (and garnets). The uppermost structural part is represented by greenish fine-grained phyllites with no recognizable minerals by the naked eye. Here, garnets are Mn-rich ($Alm_{34}Sps_{57}Prp_4Grs_5 - Alm_{66}Sps_{23}Prp_4$-$Grs_7$ from core to rim), have sub-millimetric size and contains very few inclusions of chlorite and rare epidote, quartz, and zircon; the matrix is formed by $Wmca + Chl \pm Bt \pm Pl$, where biotite and plagioclase ($X_{Ab} \sim 0.89$) are subordinate and mainly develop around garnet or in its pressure shadows. This portion of the MU preserves a few NE-dipping lens of black phyllites, with usually sharp contacts reactivated as late, brittle shear zones (Figure 3(g)). These black phyllites are characterized by a finer grain size, widespread quartz injections and are sometimes interlayered with thin ribbons of quartz-rich gray phyllites.

The Grt-Bt-micaschists are reddish-brown foliated rocks that show the same mineral assemblage of the phyllites, but with an increase in grain size. Indeed, garnet reaches millimetric dimensions, it is less spessartine-rich ($Alm_{52}Sps_{31}Prp_2Grs_{15} - Alm_{74}Sps_2Prp_6$-$Grs_{18}$ from core to rim) and contains biotite ($X_{Mg} = 0.42–0.45$) and ilmenite pre-kinematic inclusions (Figure 4(g)). Compositionally zoned plagioclase ($Ab_{85}An_{14}Or_1 - Ab_{74}An_{25}Or_1$ from core to rim) is the second type of porphyroblast after garnet; both are wrapped by a $Wmca + Chl + Bt + Qz + Ilm$ matrix oriented with the main foliation (Figure 4(g)), in which chlorite appears subordinate to biotite and grows in garnet pressure shadows or, sporadically, in the matrix as a retrograde phase.

The Grt-St-micaschists (Figure 3(h)) occur at the contact with the LAU. At the thin section scale, these rocks reveal pluri-millimetric zoned garnets ($Alm_{54}Sps_{24}Grs_{18}Prp_4 - Alm_{80}Sps_2Grs_9Prp_9$ from core to rim) with included pre-kinematic $Cld + Rt + Ilm + Mrg + Wmca \pm Qz \pm Ap \pm Zrn \pm Ep$ assemblage and wrapped by a matrix consisting of $Wmca + Chl + St + Ilm \pm Ap \pm Mnz \pm Qz \pm Pl$ (Figure 4(h)). Chloritoid ($X_{Mg} = 0.14–0.18$) has been detected as a relict phase in the matrix as well, associated to newly forming staurolite ($X_{Mg} = 0.10–0.16$). This latter occurs widespread in the matrix or concentrated around garnet porphyroblasts; chlorite and (rare) plagioclase grow in garnet pressure shadows, but retrograde chlorite also overgrows staurolite in the matrix or grows in fractures within garnets. Rutile included in garnet is commonly replaced by ilmenite, even if unaltered crystals have been detected. In the matrix, ilmenite is the main oxide, but few rutile grains are still preserved. The main foliation is marked by the orientation of ilmenite needles, chlorite and white mica flakes. Post-kinematic andalusite altered in fine-grained pinite has also been detected.

5. The intrusive complex

The intrusive complex is here referred to as both the plutons that surround the ZMC, and the dikes that directly cut the metamorphic sequence in several locations.

The plutons around the ZMC can be divided into granodiorites (more rarely tonalites), and leucocratic, medium-grained granites or microgranites. The former characterize the eastern, northern, and Northwestern sides of the ZMC and are recognizable in several roadcuts or in the slopes South-East of Zicavo. These rocks are usually highly weathered, and are composed of millimetric $Qz + Pl + Bt$. Several decimetric Mafic Microgranular Enclaves (MME) characterize the granodiorites in the area South of Zicavo, along the D69 road. In the North, near the Cozzano village, Bt-rich tonalitic rocks can also be found. The leucocratic granites are medium- to fine-grained rocks consisting of $Qz + Kfs + Pl \pm Bt \pm Wmca$ that outcrop in the slopes delimited in the West and in the North by the *Taravu* River and the *Molina* River, respectively. Locally, in the Northeastern termination of the MU, lenses of hornfelses and hornfelsed schists can be observed, directly in contact with surrounding granitoids, implying that a contact metamorphism was locally coeval with plutons intrusion, witness of the original intrusive contact between the granitoids and the ZMC. Moreover, in the eastern portion of the OU, granitoids escaping from the main pluton have been observed in the field, also suggesting the intrusive nature of the ZMC-plutons contact. However, the NW and SE sectors of the ZMC are limited by almost straight contacts: this feature could suggest the presence of NE-SW-striking faults at the boundary between the metamorphic and the plutonic rocks, as already pointed out by Rouire et al. (2014).

The dike complex is formed by various NE-SW- to N-S-striking bodies, that range from Kfs-rich leucocratic granites and/or syenites to porphyritic melanocratic granites and granodiorites. The former are well recognizable intruding the LAU and the MU, perpendicularly cutting the contact between them East of the *Mela Frisciata* locality, and outcrop in several location along the *Taravu* riverbed in the western side of the ZMC; they have cm-sized pinkish K-feldspar crystals and minor $Pl + Qz + Bt$. The porphyritic granites are mainly detectable intruding the LAU, along the Zicavo – *U Vergaju* D757a road, and consist of gray $Kfs + Pl$ phenocrysts with sparce $Bt + Qz$; they are associated with leucocratic granites. In the MU, a granodioritic dike with amphibole visible to the naked eye has been detected.

6. Tectonic and metamorphic evolution

6.1. Deformation

Based on detailed field mapping and structural overprinting criteria, three deformation phases have been

Table 1. Summary of deformation features for the three tectonic units. For each unit, the main structures related to the deformation phase are shown. A tectonic interpretation for each deformation phase is also given.

	D_1	D_2	D_3
ORTHOGNEISS UNIT	$S1_{OU}$ foliation ?	$S2_{OU}$ foliation $L2_{OU}$ lineation	$F3_{OU}$ folds
LEPTYNO-AMPHIBOLITE UNIT	$S1_{LAU}$ foliation $L1_{LAU}$ lineation	$S2_{LAU}$ foliation, $F2_{LAU}$ folds $L2_{LAU}$ lineation	$S3_{LAU}$ foliation, $F3_{LAU}$ folds
MICASCHIST UNIT	$S1_{MU}$ foliation *Top-to-the-SW thrusting and units stacking(?)*	$S2_{MU}$ foliation, $F2_{MU}$ folds *Top-to-the-SE shearing, amphibolite facies metamorphism*	$S3_{MU}$ foliation, $F3_{MU}$ folds *Brittle-ductile shearing, greenschist facies metamorphism*

discriminated (D_1, D_2, D_3) (Table 1 and Figure 5). The D_1 phase in the MU ($D_{1,MU}$), at the outcrop scale, led to development of an $S_{1,MU}$ metamorphic foliation formed by quartz-rich and phyllosilicate-rich layers (Figure 5(a)), while, at the thin section scale, microlithons and garnets' inclusion patterns highlight this $S_{1,MU}$ (Figure 4(g,h)). In the LAU, the $D_{1,LAU}$ in the metasedimentary rocks developed an $S_{1,LAU}$ that is recognizable both at the outcrop scale and as inclusions in garnet cores, or in rare microlithons in the micaschist. A NE-plunging $L_{1,LAU}$ mineralogical lineation is rarely preserved in the amphibolites through alignment of amphibole; this is associated with a top-to-the-SW sense of shear, only recognizable at the thin section scale. In the OU, the $D_{1,OU}$ related structures are not recognizable: this feature was interpreted by Thevoux-Chabuel et al. (1995) as due to the fact that the protolith of the OU was emplaced between the D_1 and the D_2 phase. However, recent U-Pb dating (458 Ma) of the orthogneiss provided by Rouire et al. (2014), and the structural similarities with the Middle Ordovician orthogneisses from Sardinia, could allow us to hypothesize a complete overprint of the $D_{1,OU}$ structures due to the $D_{2,OU}$ phase, rather than a post-D_1 emplacement of the protolith.

The main D_2 deformation occurred in a NE-SW shortening regime and is responsible for the main structures at the macro-, meso- and micro-scale, and to the overprint of D_1 structures. It is related to the development of the regional, NE-dipping S_2 axial plane foliations in the three units ($S_{2,OU}$, $S_{2,LAU}$ and $S_{2,MU}$), associated, in the LAU and the MU, with tight, NW-SE-trending, NW- to SE-plunging $F_{2,LAU}$ and $F_{2,MU}$ folds (Figure 5(b)) that affect the complex from the cm- to the map-scale. Parallel to the strike of the $S_{2,OU}$ and $S_{2,LAU}$ foliations is a NW- to SE-plunging $L_{2,OU}$ and $L_{2,LAU}$ object lineation (Figure 5(c)); this is coeval with a top-to-the-SE shearing, conspicuously observed in the entire complex, even if better expressed in the augen gneiss, through the deformation of the large quartz and/or feldspar porphyroclasts (Figure 5(d)), in the quartz injections within the black phyllites of the MU, or through asymmetric folds along the LAU-MU contact (Figure 5(e)). The D_2 phase, and the associated shearing, must have been occurred earlier than the granitoids emplacement (since granites do not show any evidence of

shearing), i.e. it must be older than 297 Ma (Rossi et al., 2012).

The D_3 phase, which deforms the D_2 structures, perhaps still occurred in a shortening regime, but showing a shortening orientation that is almost perpendicular to that of the D_2 phase (NE-SW during the D_2, NW-SE during the D_3); this phase is characterized by different scale (from outcrop to the map scale) NE-plunging $F_{3,OU}$, $F_{3,LAU}$ and $F_{3,MU}$ folds with a slight SE-vergence (Figure 5(f)), sometimes associated, in the LAU and the MU, with a NW-steeply dipping $S_{3,LAU}$ and $S_{3,MU}$ spaced crenulation cleavage. In the MU, a NE-plunging intersection lineation due to the $S_{2,MU}/S_{3,MU}$ interference can be locally recognized. D_2 and D_3 structures are locally deformed by sub-horizontal, NE-SW-trending folds. Lastly, development of NE-SW-striking, NW- to SE-dipping normal faults that displaced the complex in few locations have been described.

Shear zones − Two generations of shear zones have been possibly distinguished that could be linked to the ongoing deformation events, both discriminated by overprinting criteria.

The first generations of shear zones developed in a ductile regime during the D_2 event. They are best recognized along the two tectonic contacts which occur between the three units (Figure 2), that can be described as dextral, ductile shear zones. A top-to-the-SE sense of shear is associated to these shear zones (Figure 5(d,e)), together with a well-developed mylonitic foliation, parallel to the regional S_2, and an object lineation parallel to the strike of the foliation (NW-SE). The contact between the OU and the LAU is marked in outcrops by a mylonitic, fine-grained leucocratic body with a pervasive NE-dipping mylonitic foliation. This contact is only directly observable in a few outcrops along the Zicavo − *U Vergaju* road. The LAU-MU contact is characterized by a several meters thick ductile shear zone consisting of mylonites and, locally, ultramylonites, together with mylonitic micaschists and metavolcanics; here, the mylonitic foliation is always parallel to the NE-dipping regional S_2 in the LAU and the MU. The parallelism of the mylonitic and the regional S_2 foliation and the association of the shear component of the deformation with the regional foliation possibly allow us to ascribe the first generation of shear zones within the D_2
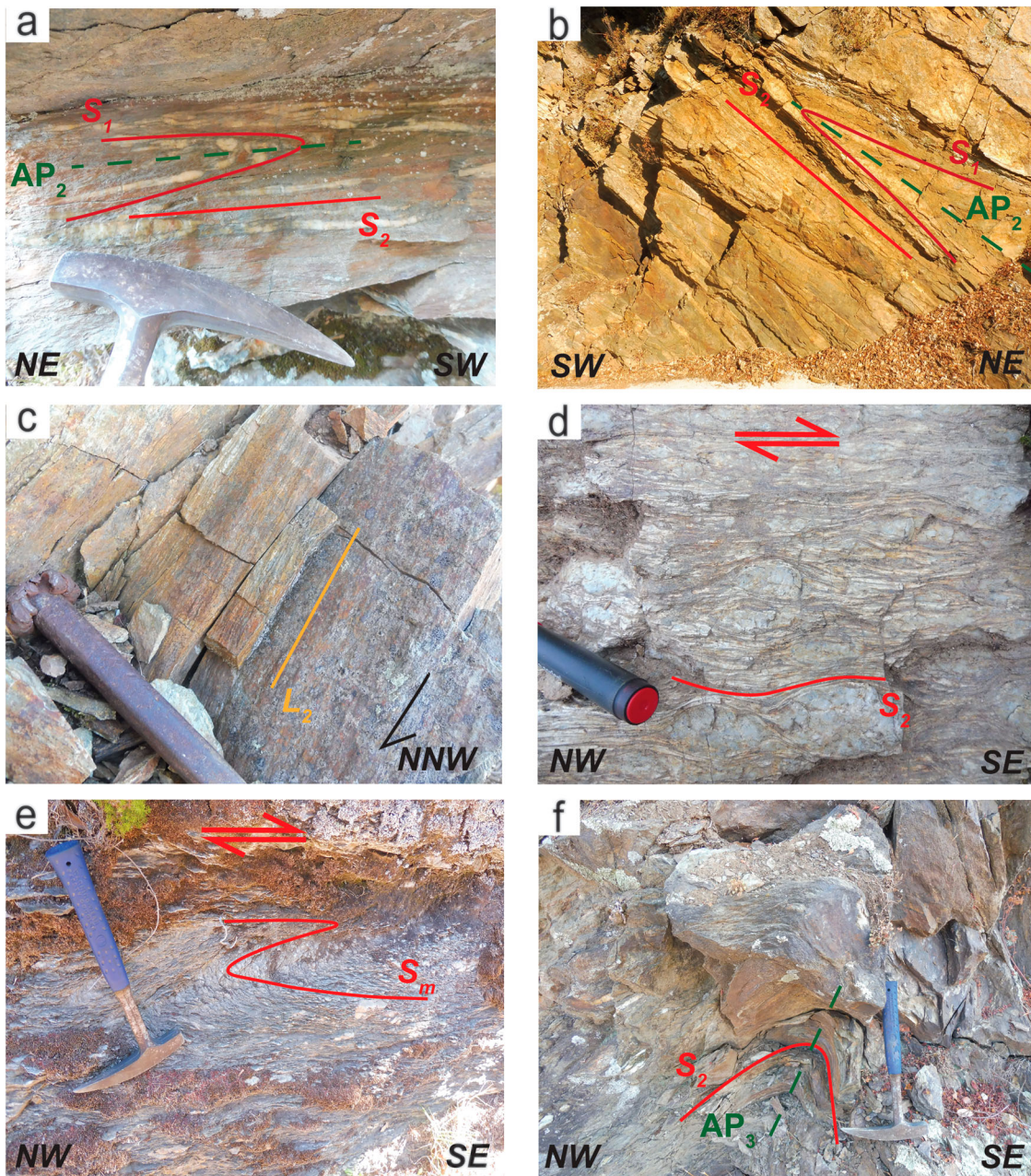
Figure 5. Mesoscopic deformational features of the ZMC. (a) Folded and transposed S_1 foliation in the MU from outcrop along the D228 road. (b) SE-plunging F_2 folds affecting the LAU along the D757a road; the former S_1 is tightly folded with an S_2 axial plane foliation development. (c) N-NW-plunging L_2 object lineation in the ultramylonitic part of the OU, North-East of locality *Rossalmu*. (d) Top-to-the-SE shear sense highlighted by a quartz porphyroclast in the mylonitic augen gneiss from the OU-LAU contact in a roadcut along the D757a road. (e) Top-to-the-SE sense of shear highlighted by an asymmetric fold in mylonites along the LAU-MU contact along the D228 road. (f) NE-plunging F_3 upright fold affecting the phyllites of the MU near the *Gierbarella* locality.

deformation phase. Furthermore, metamorphic assemblages along the mylonitic foliation (green amphibole + plagioclase and staurolite from the meta-basites and micaschists along the MU-LAU contact, respectively) are the same as the syn-D_2 assemblages away from the shear zone. It is worth noting, that, even if concentrated in these two shear zones, the shearing associated with the main foliation (S_2) in the three units is developed in the entire ZMC, and characterized by a top-to-the-SE sense of shear (Figure 4(b); Figure 5(d,e)). The second generation of shear zones is also scattered within the entire complex,

and have usually a meter-sized thickness, but can be more easily recognized and described in the MU. There, they deform the $D_{2,MU}$, and sometimes, even the $D_{3,MU}$ structures. A pervasive foliation is sometimes associated to these shear zones, parallel to an (otherwise spaced) $S_{3,MU}$ crenulation cleavage that characterize the $D_{3,MU}$. In the OU, shear bands sometimes can be detected deforming the $S_{2,OU}$ foliation at the outcrop scale.

The orogen-parallel shearing that characterizes the main deformation phase in the ZMC has been described in other septa of the Corsica Variscan

basement, for example in the Fautea-Solenzara and Porto Vecchio ones, where a dextral, transpressive shear zone (similar in kinematics to that described in the ZMC) active at *c.* 320 Ma was studied by Giacomini et al. (2008). Furthermore, similar structures have also been reported from other domains of the Variscan chain of southern Europe: in Sardinia, the Posada Asinara Shear Zone was active, with a transpressional regime, between 325/320–300 Ma (Carosi et al., 2012, 2020). Also, in the Maures Massif, the so-called Cavalaire Fault recorded a transpressional activity starting from 323 Ma (Simonetti et al., 2020). Even if robust geochronological and structural data are still needed to better evaluate a strong correlation, the dextral shearing detected and described in the ZMC could represent another witness of the widespread shearing which was active in the southern Variscides in the Middle-Upper Carboniferous.

6.2. Metamorphism

In the ZMC, a slight increase in the metamorphic grade has been observed from the NE towards the SW, that is, towards the deepest tectonic units. The metamorphic peak in the amphibolite facies, coeval with the D_2 deformation, has been constrained in the MU by occurrence of syn-$S_{2,MU}$ oriented staurolite porphyroblasts; in the LAU, staurolite has been recognized in the metapelitic intercalation, while amphibolites show the assemblage hornblende + Ca-plagioclase (andesine); staurolite and amphibole also highlight the $L_{2,LAU}$ lineations in the micaschists and amphibolites. The retrograde conditions have been qualitatively documented based on chlorite overgrowth on staurolite and biotite, or epidote and albite in the amphibolites. A comparison between two garnet-staurolite micaschists (one belonging to the MU, the other to the LAU) has been reported in Figure 6, showing the metamorphic assemblage evolution defined after microstructural relationships. Lastly, a high-temperature event is recorded in the staurolite-bearing pelitic rocks by the occurrence of post-kinematic andalusite that grows all over the matrix, at the expense of chlorite, white mica and staurolite. This HT metamorphic event is likely related to the late pluton emplacement at low pressures during the exhumation event.

A first P-T path was reported by Gardien et al. (1997) based on the petrographic descriptions provided by Thevoux-Chabuel et al. (1995); these authors described a clockwise P-T path with peak pressure in the kyanite stability field (kyanite was detected in the metapelitic intercalations of the amphibolites by Thevoux-Chabuel et al., 1995) at 0.7–0.8 GPa and ~600°C, coeval with the D_1 thickening stage, followed by a LP-HT event at 600–650°C and lower pressures, occurred during the late orogenic collapse of the complex. In this regard, more detailed petrology has been carried out in the Grt-St-micaschists from the MU (Dulcetta et al., *in preparation*). For these rocks, a preliminary clockwise P-T path is characterized by peak pressures at *c.* 1.0–1.2 GPa (at ~ 480°C), perhaps coeval with the D_1 event, and peak temperature in the amphibolite facies during the D_2 event, at lower pressures (0.6–0.8 GPa) and ~ 580–620°C. These data are slightly different in terms of temperatures from those reported by Gardien et al. (1997) and Thevoux-Chabuel et al. (1995), even if it has to mention that the two paths have been constructed for two different samples that belong to two different units.

7. Final remarks

The here presented 1:5000 geological – structural map improves the knowledge about the geology of the Zicavo area. The ZMC is formed by three tectonic units consisting of (i) orthogneiss and paragneiss (OU), (ii) metavolcanic rocks and their intercalations (LAU) and (iii) metapelites (MU). They are separated by two ductile, NW-SE-striking shear zones probably developed during the main deformation phase.

The OU is a deformed metaigneous unit formed by two types of orthogneisses (and, likely, their country rock/post-intrusion cover, the paragneiss) showing different degree of mylonitization, which increases towards the South-West. The orthogneisses from the ZMC could represent another witness of the widespread igneous activity that affected the northern Gondwana margin in the Paleozoic, as already described in the literature for the Sardinia-Corsica and the Calabria Variscan belt. Lastly, the shear deformation in the ultramylonitic orthogneiss confirms the important role of shear zones in the study area. The LAU is a bimodal metavolcanic sequence, similar to others already described in the Variscan chain. Different metasedimentary intercalations have been described, probably resulting from sediment deposition
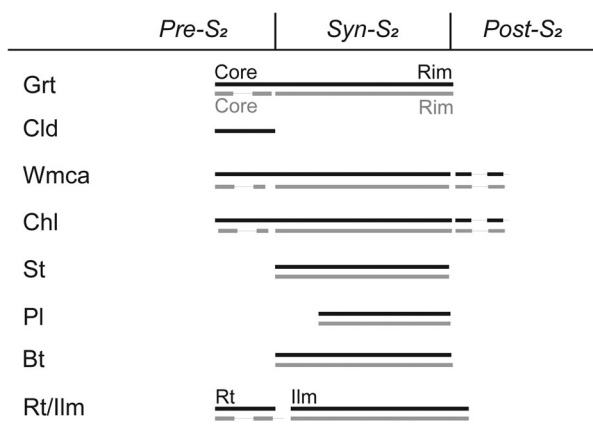

Figure 6. Metamorphic evolution scheme inferred from microstructural relationships and mineral assemblages of Grt-St micaschist from the MU (black line) and Grt-St micaschist intercalated in the LAU (gray line).

coeval with the volcanism. The serpentinite could represent a possible mantle participation to the volcanism of the LAU. The MU is a thick metapelitic sequence that tectonically overlies the LAU. As a whole, an increase in the metamorphic grade in the Zicavo complex can be inferred from NE towards the SW.

Three deformative phases have been constrained (Table 1). The D_1 phase is clearly preserved in the MU ($D_{1,MU}$) and the LAU ($D_{1,LAU}$), but it is not in the OU. The D_2 ($D_{2,OU}$, $D_{2,LAU}$ and $D_{2,MU}$) phase occurred during a NE-SW oriented shortening, under amphibolite facies conditions, leading to development of the first generation of shear zones and to the mylonitization, associated with a top-to-the-SE displacement. However, that the tectonic contacts were already formed during the D_1 as NE-dipping thrust, and were subsequently reworked assuming the present geometry cannot be completely ruled out; in this case, the badly preserved top-to-the-SW sense of shear associated with the NE-plunging $L_{1,LAU}$ lineation in the LAU could mark the transport direction associated with the stacking of the three units during the D_1. However, due to the lack of accurate data about the D_1 shearing, this must be treated as a mere hypothesis at the moment. The D_3 phase ($D_{3,OU}$, $D_{3,LAU}$ and $D_{3,MU}$) developed in early retrograde metamorphic conditions in a still shortening regime and is followed by a last, exhumation-related phase probably linked to the gravitative collapse of the complex. The second generation of shear zone can be framed within the D_3 phase, or later.

Software

The 1:5000 geological map has been drawn using the QGIS (3.26 *Buenos Aires* version) software. The final version of the Main Map, including stereographic projections of structural elements, geological cross sections, and geographic information, has been assembled within the Adobe Illustrator CC v.22 (2018) package. Structural elements have been plotted using the Stereonet$^{©}$ (*v.* 11.4.5) software.

Geolocalization

The studied area is located in southern Corsica (France), framed in the 4253/OT 'Petretto Bicchisano – Zicavo' Sheet of the IGN 1:25000 French cartographic database. The area is situated between 4636454.016–503982.706 and 4643791.001–512101.592 coordinates, WGS84 – UTM Zone 32T reference system.

Acknowledgements

Disclosure statement

No potential conflict of interest was reported by the author(s).

Funding

Data availability statement

The authors declare that all information that support the results presented in the article are provided in the text and/or in the supplemental material.

ORCID

Lorenzo Dulcetta http://orcid.org/0000-0002-0953-5437
Michel Faure http://orcid.org/0000-0003-1880-8115
Philippe Rossi http://orcid.org/0000-0003-1245-2752
Gabriele Cruciani http://orcid.org/0000-0002-6624-5655
Marcello Franceschelli http://orcid.org/0000-0002-0223-3866

References

Carmignani, L., Carosi, R., di Pisa, A., Gattiglio, M., Musumeci, G., Oggiano, G., & Pertusati, P.C. (1994). The hercynian chain in Sardinia (Italy). *Geodinamica Acta*, *7*(1), 31–47. https://doi.org/10.1080/09853111.1994.11105257

Carmignani, L., Oggiano, G., Barca, S., Conti, P., Eltrudis, A., Funedda, A., Pasci, S., & Salvadori, I. (2001). Geologia della Sardegna. Note illustrative della carta geologica della Sardegna in scala 1:200000. In: Memorie descrittive della carta geologica d'Italia LX, 283 pp. Roma: Istituto Poligrafico e Zecca dello stato.

Carosi, R., Montomoli, C., Tiepolo, M., & Frassi, C. (2012). Geochronological constraints on post-collisional shear zones in the Variscides of Sardinia (Italy). *Terra Nova*, *24*(1), 42–51. https://doi:10.1111j.1365-3121.2011.01035.x

Carosi, R., Petroccia, A., Iaccarino, S., Simonetti, M., Langone, A., & Montomoli, C. (2020). Kinematics and timing constraints in a transpressive tectonic regime: The example of the Posada-Asinara shear zone (NE Sardinia, Italy). *Geosciences*, *10*(8), 288. https://doi.org/10.3390/geosciences10080288

Cruciani, G., Franceschelli, M., Massonne, H.-J., & Musumeci, G. (2021). Evidence of two metamorphic

cycles preserved in garnet from felsic granulite in the southern Variscan belt of Corsica, France. *Lithos*, 380–381, 105919. https://doi.org/10.1016/j.lithos.2020.105919

Di Rosa, M., Frassi, C., Meneghini, F., Marroni, M., Pandolfi, L., & de Giorgi, A. (2019). Tectono-metamorphic evolution of the European continental margin involved in the Alpine subduction: New insights from Alpine Corsica, France. *Comptes Rendus Geoscience*, *351* (5), 384–394https://doi.org/10.1016/j.crte.2018.12.002

Faure, M., & Ferrière, J. (2022). Reconstructing the Variscan Terranes in the Alpine basement: Facts and arguments for an Alpidic Orocline. *Geosciences*, *12*(2), 65. https://doi.org/10.3390/geosciences12020065

Faure, M., Lardeaux, J.-M., & Ledru, P. (2009). A review of the pre-Permian geology of the Variscan French Massif Central. *Comptes Rendus Geoscience*, *341*(2-3), 202–213. https://doi.org/10.1016/j.crte.2008.12.001

Faure, M., Rossi, P., Gaché, J., Melleton, J., Frei, D., Li, X., & Lin, W. (2014). Variscan orogeny in Corsica: New structural and geochronological insights, and its place in the Variscan geodynamic framework. *International Journal of Earth Sciences*, *103*(6), 1533–1551. https://doi.org/10.1007/s00531-014-1031-8

Fossen, H. (2016). *Structural geology*. Cambridge University Press.

Gardien, V., Lardeaux, J.-M., Ledru, P., Allemand, P., & Guillot, S. (1997). Metamorphism during late orogenic extension; Insights from the French Variscan belt. *Bulletin de La Société Géologique de France*, *168*(3), 271–286.

Giacomini, F., Bomparola, R. M., Ghezzo, C., & Guldbransen, H. (2006). The geodynamic evolution of the Southern European Variscides: Constraints from the U/Pb geochronology and geochemistry of the lower Palaeozoic magmatic-sedimentary sequences of Sardinia (Italy). *Contributions to Mineralogy and Petrology*, *152* (1), 19–42. https://doi.org/10.1007/s00410-006-0092-5

Giacomini, F., Dallai, L., Carminati, E., Tiepolo, M., & Ghezzo, C. (2008). Exhumation of a Variscan orogenic complex: Insights into the composite granulitic–amphibolitic metamorphic basement of south-east Corsica (France). *Journal of Metamorphic Geology*, *26*(4), 403–436. https://doi.org/10.1111/j.1525-1314.2008.00768.x

Helbing, H., & Tiepolo, M. (2005). Age determination of Ordovician magmatism in NE Sardinia and its bearing on Variscan basement evolution. *Journal of the Geological Society*, *162*(4), 689–700. https://doi.org/10.1144/0016-764904-103

Li, X.-H., Faure, M., & Lin, W. (2014). From crustal anatexis to mantle melting in the Variscan orogen of Corsica (France): SIMS U–Pb zircon age constraints. *Tectonophysics*, *634*, 19–30. https://doi.org/10.1016/j.tecto.2014.07.021

Massonne, H.-J., Cruciani, G., Franceschelli, M., & Musumeci, G. (2018). Anticlockwise pressure-temperature paths record Variscan upper-plate exhumation: Example from micaschists of the Porto Vecchio region, Corsica. *Journal of Metamorphic Geology*, *36*(1), 55–77. https://doi.org/10.1111/jmg.12283

Paquette, J.-L., Ménot, R.-P., Pin, C., & Orsini, J.-B. (2003). Episodic and short-lived granitic pulses in a post-collisional setting: Evidence from precise U–Pb zircon dating through a crustal cross-section in Corsica. *Chemical*

Geology, *198*(1–2), 1–20. https://doi.org/10.1016/S0009-2541(02)00401-1

Passchier, C. W., & Trouw, R. A. J. (2005). *Microtectonics*. Springer Science & Business Media.

Piazolo, S., & Passchier, C. W. (2002). Controls on lineation development in low to medium grade shear zones: A study from the Cap de Creus peninsula, NE Spain. *Journal of Structural Geology*, *24*(1), 25–44. https://doi.org/10.1016/S0191-8141(01)00045-1

Rossi, P., Cocherie, A., & Fanning, C. M. (2015). Evidence in Variscan Corsica of a brief and voluminous Late Carboniferous to early Permian volcanic-plutonic event contemporaneous with a high-temperature/low-pressure metamorphic peak in the lower crust. *Bulletin de la Société Géologique de France*, *186*(2-3), 171–192. https://doi.org/10.2113/gssgfbull.186.2-3.171

Rossi, P., Lahondère, J.-C., Cocherie, A., Caballero, Y., & Féraud, J. (2012). Notice explicative, Carte géol. France (1/50 000), feuille Bastelica (1118). Orléans: BRGM, 134 p. Carte géologique par Rossi Ph., Lahondère J.-C., Loyë M.-D., Conchon O., Gauthier A. (2012).

Rossi, P., Oggiano, G., & Cocherie, A. (2009). A restored section of the "southern Variscan realm" across the Corsica–Sardinia microcontinent. *Comptes Rendus Geoscience*, *341*(2–3), 224–238. https://doi.org/10.1016/j.crte.2008.12.005

Rouire, J., Vézat, R., & Giraud, L. (2014). Carte géol. France (1/50 000), feuille Zicavo (1121), Orléans: BRGM. Notice explicative par J. Rouire, J. Gaché, Ph. Rossi (2023).

Simonetti, M., Carosi, R., Montomoli, C., Corsini, M., Petroccia, A., Cottle, J. M., & Iaccarino, S. (2020). Timing and kinematics of flow in a transpressive dextral shear zone, Maures Massif (Southern France). *International Journal of Earth Sciences*, *109*(7), 2261–2285. https://doi.org/10.1007/s00531-020-01898-6

Thevoux-Chabuel, H., Menot, R.-P., Lardeaux, J.-M., & Monnier, O. (1995). Evolution tectono-métamorphique polyphasée paléozoïque dans le socle de Zicavo (Corse-du-Sud): témoin d'un amincissement post-orogénique. *Comptes Rendus de l'Académie Des Sciences. Série 2. Sciences de La Terre et Des Planètes*, *321*(1), 47–56.

Tommasini, S. (1993). *Petrologia del magmatismo calcalcalino del Batolite Sardo-Corso: processi genetici ed evolutivi dei magmi in aree di collisione continentale e implicazioni geodinamiche* [Doctoral dissertation]. Universitá degli Studi di Firenze, 326 p.

Vézat, R. (1986). *Le Batholithe Calco-alcalin de Corse. Les formations métamorphiques calédono-varisques de Zicavo; la mise en place du batolite calco-alcalin* [Doctoral dissertation]. Université Paul Sabatier, 366 pp.

Vézat, R. (1988). Meaning of the metamorphic formations of the Zicavo area in the Mediterranean Variscan frame (Southern Corsica). *Comptes Rendus de L'Académie des Sciences Série II*, *306*(11), 725–729.

Vitale Brovarone, A., Beyssac, O., Malavieille, J., Molli, G., Beltrando, M., & Compagnoni, R. (2013). Stacking and metamorphism of continuous segments of subducted lithosphere in a high-pressure wedge: The example of Alpine Corsica (France). *Earth-Science Reviews*, *116*, 35–56. https://doi.org/10.1016/j.earscirev.2012.10.003

Whitney, D. L., & Evans, B. W. (2010). Abbreviations for names of rock-forming minerals. *American Mineralogist*, *95*(1), 185–187. https://doi.org/10.2138/am.2010.3371